

CDP-diacylglycerol phospholipid synthesis in detergent-soluble, non-raft, membrane microdomains of the endoplasmic reticulum

Mark G. Waugh,¹ Shane Minogue, Emma L. Clayton, and J. Justin Hsuan

Centre for Molecular Cell Biology, Division of Medicine, University College London, Royal Free Campus, London NW3 2PF, United Kingdom

Abstract Phosphatidylinositol (PI) is essential for numerous cell functions and is generated by consecutive reactions catalyzed by CDP-diacylglycerol synthase (CDS) and PI synthase. In this study, we investigated the membrane organization of CDP-diacylglycerol synthesis. Separation of mildly disrupted A431 cell membranes on sucrose density gradients revealed cofractionation of CDS and PI synthase activities with cholesterol-poor, endoplasmic reticulum (ER) membranes and partial overlap with plasma membrane caveolae. Cofractionation of CDS activity with caveolae was also observed when low-buoyant density caveolin-enriched membranes were prepared using a carbonate-based method. However, immunoisolation studies determined that CDS activity localized to ER membrane fragments containing calnexin and type III inositol (1,4,5)-trisphosphate receptors but not to caveolae. Membrane fragmentation in neutral pH buffer established that CDP-diacylglycerol and PI syntheses were restricted to a subfraction of the calnexin-positive ER. In contrast to lipid rafts enriched for caveolin, cholesterol, and GM1 glycosphingolipids, the CDS-containing ER membranes were detergent soluble. In cell imaging studies, CDS and calnexin colocalized in microdomain-sized patches of the ER and also unexpectedly at the plasma membrane. **These results demonstrate that key components of the PI pathway localize to nonraft, phospholipid-synthesizing microdomains of the ER that are also enriched for calnexin.**— Waugh, M. G., S. Minogue, E. L. Clayton, and J. J. Hsuan. CDP-diacylglycerol phospholipid synthesis in detergent-soluble, non-raft, membrane microdomains of the endoplasmic reticulum. *J. Lipid Res.* 2011. 52: 2148–2158.

Supplementary key words beta-oxidation • diabetes • fatty acid/metabolism • insulin resistance • obesity

There is a large body of literature supporting the idea of lateral lipid segregation at the plasma membrane,

M. G. W. and S. M. acknowledge support from the Biotechnology and Biological Sciences Research Council (BBSRC) (grant BB/G021163/1) and Royal Free Hospital National Health Service (NHS) Trust support for the advanced microscopy unit and the Centre for Biomedical Sciences (J.J.H.). E. L. C acknowledges support from the Peter Samuel Royal Free fund.

Manuscript received 8 June 2011 and in revised form 14 September 2011.

Published, JLR Papers in Press, September 21, 2011

DOI 10.1194/jlr.M017814

trans-Golgi network, and endosomes, with a particular focus on the characterization and functions of cholesterol- and glycosphingolipid-enriched membrane microdomains often referred to as lipid rafts (1, 2). Much less is known about possible membrane domain organization at the endoplasmic reticulum (ER), which is the largest cellular membrane structure and also the principal site for cellular phospholipid synthesis (3). Particular regions of the ER that form contacts with mitochondria [reviewed in (4)], usually referred to as mitochondria-associated membranes (MAM), are known to be major sites for cellular phosphatidylserine, phosphatidylcholine, and phosphatidylethanolamine production (5). There are reports that MAMs contain detergent-insoluble membrane microdomains (6, 7) analogous to plasma membrane rafts, and that MAMs are enriched for molecular chaperones such as calnexin (8) as well as signaling molecules such as type III inositol (1,4,5)-trisphosphate receptors (IP₃R) (9, 10). This has led to the proposal that MAMs represent important sites for the compartmentation and regulation of intracellular Ca²⁺ release (10), a key event in phosphatidylinositol (PI)-dependent, phospholipase C (PLC) signaling. However, the intramembrane distributions of enzymes involved in the synthesis of PI and its precursor, CDP-diacylglycerol (CDP-DAG), at the ER have not yet been characterized in detail.

The cellular localization and possible compartmentation of processes involved in the provision of PI for receptor-stimulated PLC signaling have been widely debated (11–14). In a classical, simplified model for phosphoinositide signaling, agonist activation of G protein-coupled and tyrosine kinase receptors occurs at the plasma membrane

Abbreviations: CDP-DAG, CDP-diacylglycerol; CDS, CDP-diacylglycerol synthase; ER, endoplasmic reticulum; IP₃R, inositol 1,4,5-trisphosphate receptor; MAM, mitochondria-associated membrane; PA, phosphatidic acid; PI, phosphatidylinositol; PI(4,5)P₂, phosphatidylinositol 4,5-bisphosphate; PI4P, phosphatidylinositol 4-phosphate; PLC, phospholipase C; PNS, postnuclear supernatant.

¹To whom correspondence should be addressed.

e-mail: m.waugh@ucl.ac.uk

Copyright © 2011 by the American Society for Biochemistry and Molecular Biology, Inc.

This article is available online at <http://www.jlr.org>

and leads to the rapid PLC-catalyzed hydrolysis of PI 4,5-bisphosphate [PI(4,5)P₂] into the second messenger molecules DAG and inositol (1,4,5)-trisphosphate (IP₃). The IP₃ then diffuses and is free to bind IP₃R. These are large transmembrane channel proteins, which in the tetrameric ligand-activated state, facilitate the release of Ca²⁺ sequestered in the ER. In order to sustain high levels of signaling through PLC, PI(4,5)P₂ must be resynthesized via PI and PI 4-phosphate, and radiolabeling studies have pointed toward the existence of agonist-sensitive and insensitive metabolic pools of PI and possibly a closed cycle of intermediates (11, 15).

In contrast to the large body of literature on receptor-dependent phosphoinositide signaling, much less information is available on the metabolic pathways and mechanisms involved in PI synthesis. In ER membranes (16), phosphatidic acid (PA), formed following the phosphorylation of DAG by DAG kinase, is condensed with CTP to produce CDP-DAG in a reaction catalyzed by CDP-DAG synthase (CDS) (17). The CDP-DAG liponucleotide can then undergo PI synthase-catalyzed headgroup exchange with inositol to form PI (18). Although PI synthesis has been reported to occur in the plasma membrane (19, 20) and to a lesser extent in the Golgi (21), it is generally accepted that similar to IP₃Rs, the ER is the primary site for the synthesis of both PI and CDP-DAG [reviewed in (17, 18)]. In concordance with this view, the single human PI synthase enzyme (22) and the major CDS isozyme have been demonstrated to be ER proteins (23–26). Interestingly, despite large fluxes in intracellular Ca²⁺ concentrations during PLC signaling, there are demonstrations that both CDS and PI synthase are inhibited by Ca²⁺ in the micromolar to millimolar to mM range (27–29). Moreover, increasing the levels of either CDS or PI synthase by overexpression of the recombinant enzymes induces disproportionately small increases in the cellular levels of their phospholipid products (22). Hence, it is not clear how the ER localization and Ca²⁺ sensitivity of CDS and PI synthase are compatible with the repletion of their lipid products following receptor activation.

Although both PI and IP₃R localize primarily to the ER, there are independent studies showing that these molecules can also be found in plasma membrane caveolae (30, 31). One possible inference from such studies is that plasma membrane rafts contain a pool of PI and IP₃R important for phosphoinositide signaling. However, the impurity of caveolae raft preparations (32, 33) and the recent identification of detergent-insoluble, raft-like, ER membrane domains (7, 34) suggest that a more thorough characterization of the compartmentation of these important signaling molecules is necessary.

This study utilizes different subcellular fractionation techniques combined with immunoisolation of ER membrane domains and confocal immunofluorescence microscopy to establish that a pool of calnexin and IP₃R localize to noncaveolar, buoyant, ER subdomains which are also hotspots for PI and CDP-DAG synthesis. These membrane domains have biochemical properties consistent with the phospholipid-rich, nonraft, ER membrane domains predicted by Shaikh and Edidin (35).

Materials

Secondary antibodies, [^α-³²P]CTP (20mCi/ml), [³H]Inositol with PT6–271 stabilizer (17.1Ci/mmol), prestained molecular weight markers, Protein G Sepharose 4 Fast Flow, and the ECL Western blotting detection system were purchased from GE Healthcare (Little Chalfont, Buckinghamshire, UK). Anti-caveolin, anti-p115, and anti-IP₃R (type III) antisera were obtained from BD Biosciences (Oxford, UK). Anti-CDS1 was bought from AbD Serotec. Anti-calnexin antiserum was purchased from Assay Designs and Stressgen (Ann Arbor, MI). Cell culture reagents and the Amplex Red cholesterol Assay kit were from Life Technologies (Paisley, UK). Protease inhibitor cocktail tablets (Complete™, without EDTA) were from Roche Diagnostics (Burgess Hill, West Sussex, UK). All other reagents were obtained from Sigma-Aldrich (Poole, Dorset, UK).

Cell culture, radiolabeling, and analysis of phosphoinositide lipids

A431 cells were maintained at 37°C in a humidified incubator at 10% CO₂. Cells were cultured in DMEM supplemented with Glutamax, 10% fetal calf serum, 50 i.u./ml penicillin, and 50 µg/ml streptomycin. Standard methods were used for the analysis of [³H]inositol-labeled phosphoinositides (32). A431 cells were cultured in inositol-free medium containing 1% fetal calf serum in the presence of 2 µCi/ml [³H]inositol for 48 h. Following subcellular fractionation, membrane fractions (100 µl) were extracted with an equal volume of chloroform-methanol-1M HCl (60:36:4). Samples were vortexed and centrifuged for 10 s in a microcentrifuge at 10,000 rpm. Organic phases were collected and reextracted with methanol-1M HCl (1:1). Samples were vortexed and centrifuged as before and the organic phase from each tube collected. Lipids were resolved by TLC on Silica-60 plates (Merck), which had been pretreated with 1% potassium oxalate, 2 mM EDTA in 50% methanol and developed using an acid solvent system composed of propan-1-ol:2 M acetic acid (65:35) containing 1% 5M H₃PO₄. TLC plates were then imaged using a Typhoon 9400 phosphorimager (GE Healthcare).

Subcellular fractionation of A431 cells

For these experiments, 2–4 confluent 15 cm dishes of A431 cells were used. Protein loading of the gradients was measured as 6.6 ± 2.3 mg (mean ± SEM, n = 3) and lipid loading was 188.3 ± 33.6 (n = 3) µmoles cholesterol/mg protein. The method used for subcellular fractionation was essentially the same as that described by Sillence and Downes (36) with some minor modifications. A431 cells were harvested on ice in 0.25 M sucrose, 10 mM EGTA, 10 mM EDTA, 20 mM Tris-HCl, pH 7.4 and homogenized by 15 strokes using a hand-held Dounce homogenizer. A postnuclear supernatant (PNS) was obtained by centrifugation at 2,000 rpm for 5 min in a bench-top centrifuge. All subsequent steps were carried out on ice or at 4°C. The resulting nuclear pellet was rehomogenized and another PNS obtained. The PNSs from both clearing steps were combined and loaded onto a 10 ml continuous 24–50% sucrose gradient formed in an ultracentrifuge tube using the pump and gradient mixing system from an SMART separation unit (GE Healthcare). Following centrifugation for 16–18 h at 35,000 rpm (151,000 g) in a Beckman SW41 Ti rotor, 1 ml samples were collected starting from the top of the tube for further analyses. Refractive index measurements of individual gradient fractions were determined with a Leica AR200 refractometer and these values were converted to sucrose densities using linear regression and standard conversion tables (37).

Isolation of caveolin-rich buoyant membrane domains from A431 cells

Caveolin-rich buoyant membrane domains were prepared using a detergent-free method as previously described (32). All procedures were carried out at 4°C. A431 cell monolayers grown to confluence in 15 cm dishes were washed twice with phosphate-buffered saline and scraped into 2 ml of 100 mM Na₂CO₃, pH 11.0 containing COMPLETE protease inhibitors, 10 mM EGTA, and 10 mM EDTA. Cells were disrupted by sonication (6 × 10 s bursts) using a Soniprep 150 sonicator (MSE) on setting 10–12. Sonicated cells (2 ml) were mixed with 2 ml of 90% (w/v) sucrose in MBS buffer (25 mM Mes, 150 mM NaCl, pH 6.5) and placed in a 12 ml ultracentrifuge tube. A 5–35% (w/v) discontinuous sucrose gradient was formed above the sample by layering on 4 ml of 35% (w/v) sucrose solution followed by 4 ml of 5% (w/v) sucrose solution. The sample was then centrifuged at 39,000 rpm (175,000 g) for 16–18 h in a Beckman SW41 Ti rotor. A thin band of membrane was identified at the 5–35% (w/v) sucrose interface that was enriched in caveolin but excluded the bulk of the cellular protein (38). One milliliter fractions were collected from the top of each gradient.

In some experiments, as an assay for resistance to detergent solubilization, the detergents 10 mM β-octylglucoside and 4 mM deoxycholate were added to the sodium carbonate sonication buffer (39).

Fractionation of A431 sonicated cell membranes in neutral pH buffer

A431 cells were harvested by scraping into neutral pH buffer consisting of 0.25 M sucrose, 10 mM EGTA, 10 mM EDTA, 20 mM Tris-HCl, pH 7.4 containing COMPLETE protease inhibitors and probe sonicated by 3 × 5 s bursts with a Vibra-cell probe (Sonics) sonicator at amplitude setting 40 operated in pulsed mode. This sonicated fraction was transferred to a 12 ml polycarbonate ultracentrifuge tube (Beckman) and adjusted to 45% (w/v) sucrose by the addition of an equal volume of 90% (w/v) sucrose in 10 mM Tris-HCl, pH 7.4, 1 mM EDTA, 1 mM EGTA to give a final volume of 4 ml. The sample was overlaid with 2 ml of 35% (w/v) sucrose, 2 ml of 20% (w/v) sucrose followed by 4 ml of 5% (w/v) sucrose, and subjected to discontinuous equilibrium sucrose density gradient centrifugation overnight at 4°C at 180,000 g using a swing-out SW41 Beckman rotor. One milliliter gradient fractions were then harvested beginning from the top of the tube and stored at –20°C.

Immunoblotting of A431 cellular fractions

Samples from sucrose gradient fractions were mixed with an equal volume of 2× sample buffer and 40 μl samples separated by SDS-PAGE. Proteins were transferred to Immobilon-P membranes (Millipore) and probed with various antibodies. Bound antibody was detected using the ECL system. Western blots were quantified by densitometric analyses using image analysis software in Adobe Photoshop CS4.

Immunoprecipitation of caveolae and calnexin-rich domains

Caveolae were immunisolated as described previously (40). For the isolation of calnexin-containing membranes, samples were precleared with 20 μl Protein G Sepharose beads for 1 h at 4°C. Cleared samples were incubated for 2 h at 4°C with anti-caveolin antiserum (10 μl/ml), which had been prebound to Protein G Sepharose. Immunocomplexes were collected by centrifugation and washed four times with 20 mM Tris-HCl, pH 7.4.

CDS assays

CDS activity was assessed by measuring the incorporation of radiolabeled CTP into PA to form the liponucleotide

[³²P]CDP-DAG (40). Fifty microliter samples from each gradient fraction were mixed with an equal volume of assay buffer composed of 20 mM Tris-HCl pH 7.4, 40 mM MgCl₂, 2 mM EGTA, and 20 μCi/ml [³²P]CTP. Where indicated, exogenous PA was added as a substrate for CDS to a final concentration of 0.5 mM. Samples were incubated at room temperature for 30 min. Reactions were terminated and organic phases were extracted by the addition of an equal volume of chloroform-methanol-1M HCl (60:36:4). Samples were vortexed and centrifuged for 10 s in a bench-top centrifuge at 10,000 rpm. Organic phases were collected and reextracted with methanol-1M HCl (1:1), vortexed and centrifuged as before, and the organic phase from each tube collected. Lipids were resolved by TLC on Silica-60 plates (Merck), which had been pretreated with 1% w/v potassium oxalate, 2 mM EDTA in 50% methanol and developed using an acid solvent system composed of propan-1-ol:2M acetic acid (65:35) containing 1% 5M H₃PO₄. TLC plates were then exposed to X-ray film to visualize radiolabeled CDP-DAG. The amount of radioactivity associated with each spot identified by TLC was determined by counting Cerenkov radiation.

PI synthase assays

PI synthase activity was assayed by mixing equal volumes of sample (50 μl) with assay buffer to give a final composition of 10 mM Tris-HCl pH 7.4, 10 mM MgCl₂, 1 mM EGTA, 1 mM CTP, and [³H]inositol (1–2 μCi/tube). It should be noted that 1 mM CTP was included to enable substrate CDP-DAG to be produced from endogenous PA. Samples were incubated for 1 h at 37°C and reactions were terminated by the addition of an equal volume of chloroform-methanol-1M HCl (60:36:4). Lipids were then extracted and analyzed by TLC as described for the analysis of CDP-DAG synthesis. TLC plates were then sprayed with ENHANCE™ to allow the visualization of radiolabeled phospholipids. Following fluorography, the identity of radiolabeled lipid spots was determined by comparison with nonradiolabeled lipid standards visualized by iodine staining. The amount of radioactivity associated with each spot was determined by scraping spots off the TLC plates and liquid scintillation counting. Alternatively, each organic phase was counted directly by liquid scintillation counting where TLC analysis revealed that [³H]PI was the only radiolabeled lipid produced in the assay.

Cholesterol mass assays

The cholesterol content of equal volume membrane fractions (50 μl) was assayed using the Amplex Red cholesterol assay kit from Molecular Probes (Life Technologies, Paisley, UK).

Detection of GM1 glycosphingolipid

A dot blotting method was employed to establish the gradient distribution of GM1 glycosphingolipid (41). Equal volume 1 μl samples of each subcellular fraction were dotted onto nitrocellulose membrane and probed with HRP-conjugated cholera toxin B subunit (1:10,000) to detect GM1 glycosphingolipid using ECL reagents.

Confocal immunofluorescence microscopy

COS-7 cells were grown on poly(L)lysine-coated glass coverslips for 24 h, fixed with 4% (v/v) formaldehyde for 10 min on ice, permeabilized by treatment with –25°C methanol for 2 min (42), then immunostained with anti-calnexin and anti-CDS. After counterstaining with Hoechst 33342 (Life Technologies), the coverslips were mounted in ProLongGold anti-fade reagent (Life Technologies). Cells were imaged as described previously (42) using a Zeiss LSM 510 Meta laser-scanning confocal microscope system.

RESULTS

Cofractionation of CDS and PI synthesis with IP₃R and calnexin and to a lesser degree with caveolin

CDS and IP₃R function at different ends of the phosphoinositide dependent signaling cascade but are both known to localize primarily at the ER. However, it is not known if both CDS and IP₃R localize to the same ER membrane regions. To address this issue, we determined the subcellular distribution of CDS activity and IP₃R in A431 cells using a subcellular fractionation scheme that involves disruption of cells by Dounce homogenization in neutral pH buffer (36). Postnuclear supernatants prepared from

such cell homogenates were centrifuged in a continuous 24–50% (w/v) sucrose density gradient (Fig. 1). This procedure separates different organelles on the basis of their equilibrium buoyant density, a physical property largely determined by organelle-specific protein:lipid ratios. Equal volume samples from each gradient fraction were subsequently assayed for CDS activity (Fig. 1A) using endogenous membrane PA as the lipid substrate. In separate experiments using the same subcellular fractions, the synthesis of PI was measured using endogenous membrane-associated CDP-DAG and exogenous [³H]inositol as substrates for PI synthase (Fig. 1B). Note that a high concentration of CTP (1 mM) was included in the PI synthase

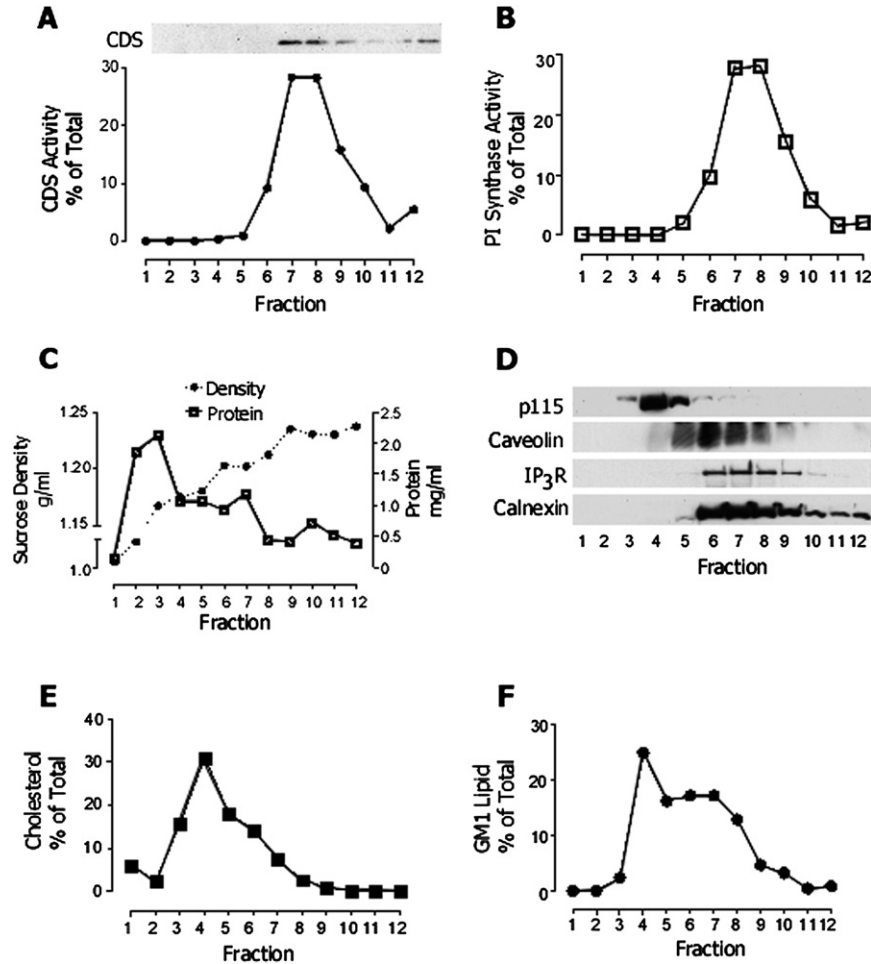


Fig. 1. CDS activity cofractionates with type III IP₃R, calnexin and PI synthase. A431 cells were homogenized in neutral pH buffer and the PNSs subjected to ultracentrifugation on a 10 ml, 20–50% continuous sucrose gradient. Fractions 1 and 2 correspond to the loading layer and fraction 12 corresponds to the densest fraction. One milliliter fractions were collected beginning at the top of the gradient for analyses. **A:** Gradient distribution of CDS enzyme determined by immunoblotting and CDS-catalyzed [³²P]CDP-DAG (total 129,311 cpm) generation using endogenous PA and added [³²P]CTP as substrates. **B:** Distribution of [³H]PI generation (total of 51,444 dpm) catalyzed by PI synthase using endogenous membrane-associated CDP-DAG and added [³H]inositol as substrates. **C:** Protein content of the gradient fractions as determined by the Bradford assay and sucrose density of the gradient fractions as measured by refractometry. **D:** Immunoblots showing the gradient distributions of p115, a marker protein for the Golgi apparatus, caveolin, a marker protein for plasma membrane caveolae, the ER proteins IP₃R and also CDS. **E:** Distribution of cholesterol in the gradient fractions as measured by the Amplex Red cholesterol assay. **F:** Distribution of GM1 glycosphingolipid in the gradient fractions as detected by dot-blotting with HRP-conjugated cholera toxin B subunit. Data are representative of at least two independent determinations from three separate subcellular fractionation experiments.

assays in order to maintain membrane levels of CDP-DAG. Using these methodologies, both CDS and PI synthase activity manifested as broad peaks in fractions 7 and 8 of the sucrose gradient corresponding to a sucrose density of 1.2–1.23 g/ml (Fig. 1C). Because these assays utilize membrane associated lipids and enzymes, it is possible to infer that both the CDS and PI synthase enzymes can access PA and CDP-DAG phospholipids in these membrane fractions. The gradient distribution of CDS activity closely paralleled that of CDS protein as determined by anti-CDS immunoblots (Fig. 1A), thus demonstrating that CDP-DAG synthesis reported the gradient distribution of the CDS enzyme.

Comparison of the distribution of CDS activity with Western blots directed against different subcellular membrane markers (Fig. 1D) demonstrated that CDS activity was well resolved from the Golgi-associated protein p115 but partially overlapped with immunoreactivity for caveolin. Caveolin is a protein marker for cholesterol-enriched plasma membrane caveolae (43, 44) and is also present at the *trans*-Golgi network (45) and to a lesser degree on ER membranes (46). Additionally, we investigated the gradient distributions of the established ER-resident calcium binding lectin calnexin and type III IP₃R calcium release channels (8–10). Immunoreactivity for both proteins substantially cofractionated in fractions 6 to 10 (Fig. 1A), which is also the region of the gradient to where both CDP-DAG and PI synthesis were localized.

Measuring the distribution of the lipid raft-associated lipids cholesterol (Fig. 1E) and GMI glycosphingolipid (Fig. 1F) revealed that the peak distributions for both molecules were in the buoyant fractions 4 and 5 (1.17–1.18 g/ml sucrose) corresponding to the Golgi and plasma membrane-enriched region of the gradient. Moreover, and particularly in the case of cholesterol, there was very little overlap with the gradient distributions of either CDS or PI synthase activities. Hence, subcellular fractionation following mild homogenization demonstrated that both PI synthase and CDS activities cofractionated with cholesterol-poor, dense, ER membranes but also raised the possibility that a minor pool of both enzymes could be localized at least partly to more buoyant caveolae membranes.

CDS activity in noncaveolar buoyant membrane domains of the ER

Our initial density gradient analyses revealed partial overlap between caveolin, CDS activity, and IP₃R, leading to the possibility that subpopulations of these primarily ER proteins may also colocalize in caveolae. Alternatively, as some caveolin protein has been found associated with ER membranes (46), there was a possibility that CDP-DAG synthesis and IP₃R localized to an ER fraction that also contained caveolin. We investigated these scenarios using an established detergent-free method to isolate caveolin-enriched low buoyant density membranes (38) followed by the immunoisolation of intact caveolae from this membrane preparation (32, 47).

As a first step to isolate caveolae membranes, A431 cells were scraped into a sodium carbonate buffer, sonicated to

disrupt membranes, and fractionated on a 45–35–5% (w/v) sucrose step gradient (38). In common with other groups and in concordance with our previous work (38, 48), we found that the low buoyant density membranes (1.01–1.06 g/ml sucrose) found in fractions 4, 5, and 6 of the step gradient were enriched in caveolin protein (Fig. 2A, B). Furthermore, these buoyant membranes contained little of the total cellular protein (Fig. 2A). We have previously shown (49) that carbonate addition leads to the isolation of membranes with a high lipid-protein ratio due to removal of peripheral membrane protein but not phospholipids (32, 39, 50, 51) by alkaline pH during the cell disruption step (51). When CDS activity was assayed across the gradient fractions, the distribution was found to closely parallel that of caveolin with activity concentrating in the caveolin-enriched fractions (Fig. 2D). When the distributions of IP₃R and calnexin were determined by Western blotting, subpopulations of both proteins were detected in the caveolin-rich buoyant membrane fraction (Fig. 2B, C). However, quantitative analysis of the immunoblots revealed that a substantial pool of IP₃R also localized to fractions 10–12 in the dense region of the gradient (Fig. 2C), thereby indicating a degree of heterogeneity in terms of ER membrane biophysical properties. This heterogeneity, apparent in the distribution of membrane regions with different buoyant densities, was particularly clear when comparing the gradient distributions of CDS activity and IP₃R (Fig. 2D). Typically, 80–90% of the total cellular [³²P] CDP-DAG generation was associated with the buoyant fractions 4–6 compared with just 40–60% of the cellular IP₃R or calnexin contents.

Given that CDP-DAG synthesis was targeted to the buoyant fraction and that this phospholipid is a metabolic precursor to PI, we extended our analyses to investigate the distribution of PI synthase activity. Assaying for [³H]PI generation in the membrane fractions revealed that the distribution of PI synthase activity did indeed closely parallel that of [³²P]CDP-DAG production (Fig. 2E), suggesting that the enzymes and lipid substrates required for phosphatidylinositol synthesis are present within the same buoyant-membrane fraction that also contains caveolae lipid rafts.

It remained possible that sonication in sodium carbonate had caused substantial fusion of ER and plasma membranes or alternatively, that calnexin and CDS localized to caveolae rafts. However, both of these scenarios were discounted by the finding that under conditions known to clear 70–100% of the cellular caveolae (32), we did not detect substantial coimmunoprecipitation of either CDS activity or calnexin with immuno-purified caveolae (Fig. 2F). These analyses also showed that the CDS and calnexin were targeted to noncaveolar membrane domains. This finding prompted us to consider the possibility of immunisolating the buoyant ER membranes present in the caveolin-rich buoyant membrane fraction. Using a polyclonal antiserum directed against the carboxy-terminus of calnexin, it was possible to isolate membranes containing the target antigen calnexin along with both IP₃R and CDS activity (Fig. 3). Taken together, these results established that calnexin, CDS, and IP₃R proteins were colocalized within the same ER

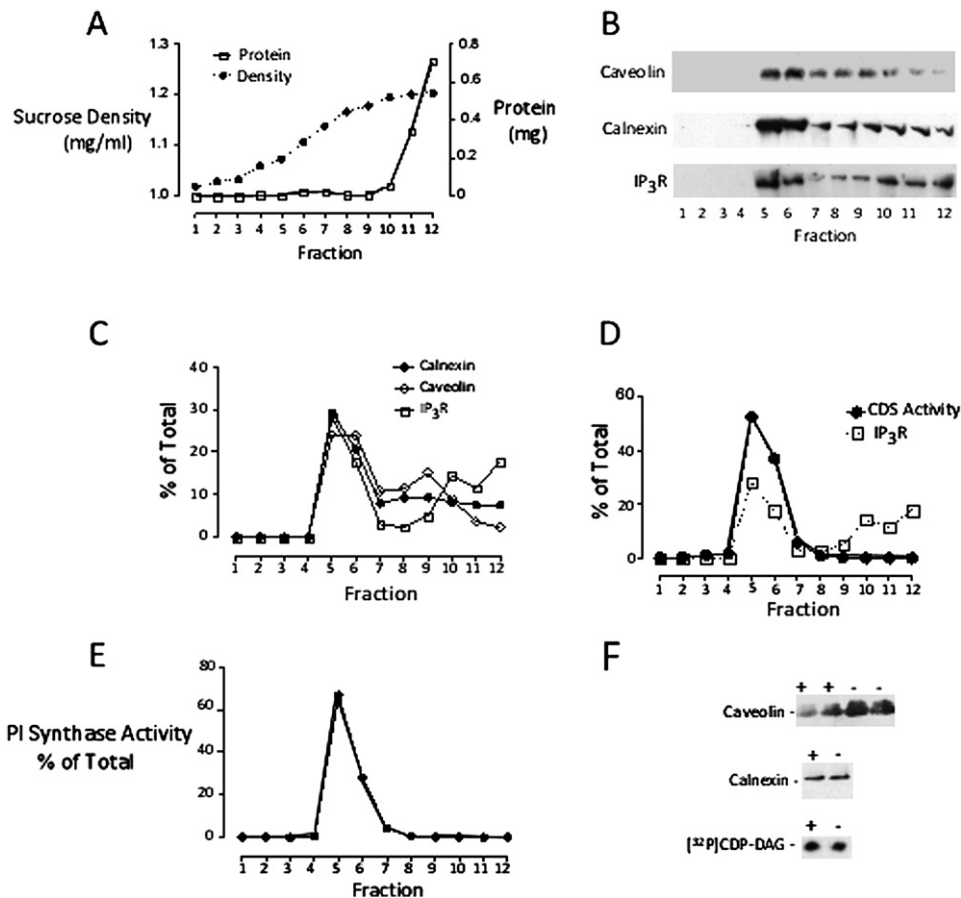


Fig. 2. CDP-DAG and PI generation in a caveolin-rich buoyant membrane fraction but not in immunoprecipitated caveolae. A431 cells were sonicated in the presence of 0.1 M sodium carbonate, pH 11.0 and the homogenate centrifuged in a discontinuous sucrose density gradient. Fractions 5 and 6 correspond to the interface of the 5 and 35% sucrose layers. A: Protein content of the gradient fractions as determined by the Bradford assay and sucrose density of the gradient fractions as measured by refractometry. B: Immunoblots demonstrating the gradient distributions of caveolin, calnexin, and IP₃R. C: Densitometric analysis comparing the distributions of caveolin, calnexin, and IP₃R in the gradient fractions. D: Distribution of CDS activity (total cpm 32,517) as measured using α [³²P]CTP and endogenous PA as substrates for the enzyme compared with the distribution of IP₃R. E: Distribution of [³H]PI synthesis (total dpm 450,094) in the gradient F: Caveolae were immunoprecipitated from the caveolin-enriched buoyant fractions 5 and 6 using established methods and equal volumes of the caveolae depleted supernatants (+ lanes) or control (- lanes) analyzed by immunoblotting for caveolin and calnexin content, or endogenous CDS activity. The results presented here are representative of three independent experiments.

membrane domain and also that a widely used technique to isolate caveolin-enriched membranes also contains buoyant raft-like ER membranes.

CDS and PI synthase activities localize to a subfraction of the calnexin containing ER membrane

Due to the removal of peripherally associated proteins (51) it was not possible to infer from the carbonate gradient results that PI and CDP-DAG syntheses were compartmentalized within the ER. This led us to modify our membrane fractionation scheme and to carry out the experiment in the absence of carbonate at neutral pH while retaining the probe sonication step, which we have shown previously to result in the formation of membrane vesicles in the 50–250 nm diameter size range (32, 48, 49). Using this approach, we observed almost identical gradient distributions of CDP-DAG and PI generation (Fig. 4A, B). However, there

were substantial differences in the gradient distributions of PI and CDP-DAG synthesis versus both calnexin and IP₃R (Fig. 4C, D). Under these conditions, a peak of CDS and PI synthase activity cofractionated with a buoyant fraction of calnexin and IP₃R. Conversely, very little CDP-DAG and PI synthesis was measured in fractions 9–12 corresponding to the 45% sucrose layer and which contained 60–70% of the total ER membrane-associated calnexin and IP₃R. From these results, we deduce that most of the cellular CDS and PI synthase activities localize to a subfraction of the calnexin containing ER membrane.

CDS localizes to detergent-soluble membrane domains distinct from cholesterol-rich lipid rafts

We next investigated whether the CDS-enriched ER membrane fractions shared properties other than buoyancy with plasma membrane rafts. Resistance to detergent

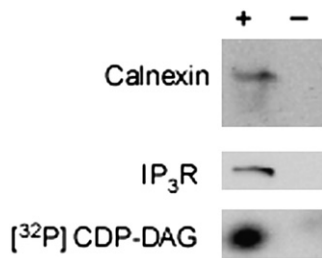


Fig. 3. Coimmunoprecipitation of CDS activity, calnexin, and IP₃R on intact membranes from the buoyant fraction. Anti-calnexin immunocomplexes (+) and control samples (-) isolated from caveolin-rich buoyant membrane fractions were bound to Protein G Sepharose beads and analyzed by immunoblotting for the presence of calnexin and IP₃Rs. [³²P]CDP-DAG generation was detected by CDS enzyme assays carried out on intact membrane domains immunisolated on beads using endogenous PA as substrate. Figure shows an image obtained from a TLC autoradiograph used to detect [³²P]CDP-DAG. Data are representative of three independent experiments.

solubilization is a characteristic property of membrane rafts; hence, we investigated the gradient distribution of CDS activity in membranes prepared in the presence of β -octylglucoside (10 mM) and deoxycholate (4 mM), a detergent mix which, unlike Triton X-100, does not result in significant solubilization of acidic phospholipids (52) or inhibition of CDS activity (53). In these gradients, a significant proportion of the cellular caveolin content was detected in the low buoyant density (1.06–1.1 g/ml sucrose)

detergent resistant membranes fractions 4–6 (**Fig. 5A, B**), and was well resolved from calnexin, which localized to the dense (1.19–1.2 g/ml sucrose) region of the gradient. These buoyant fractions contained little of the total cellular protein content (**Fig. 5C**) but were particularly enriched in the raft lipids cholesterol and GM1 glycosphingolipid (**Fig. 5D, G**). In contrast to the raft lipids and caveolin, the CDS enzyme, in common with calnexin, was localized to the dense region of the gradient (**Fig. 5E**). This dense region of the gradient also contained a pool of PI, PI4P, and PI(4,5)P₂ phospholipids (**Fig. 5F**) but was practically devoid of either cholesterol or GM1 lipids, which are known to be enriched in lipid rafts. This led us to infer that the CDS-containing ER membrane microdomains described here are biochemically different in terms of their lipid content and detergent solubility to plasma membrane lipid rafts.

Imaging CDS distribution in the ER

We employed confocal immunofluorescence microscopy to investigate whether the CDS and calnexin-rich ER domains could be distinguished from the bulk of the ER. The intracellular localizations of calnexin and CDS were imaged by immunofluorescence staining of cells, which were permeabilized in -20°C methanol in order to preserve ER membrane architecture (**Fig. 6**). These experiments revealed extensive staining of a reticular network of intracellular membranes, which is characteristic of localization to the ER (**Fig. 6, detail 1**). Most strikingly,

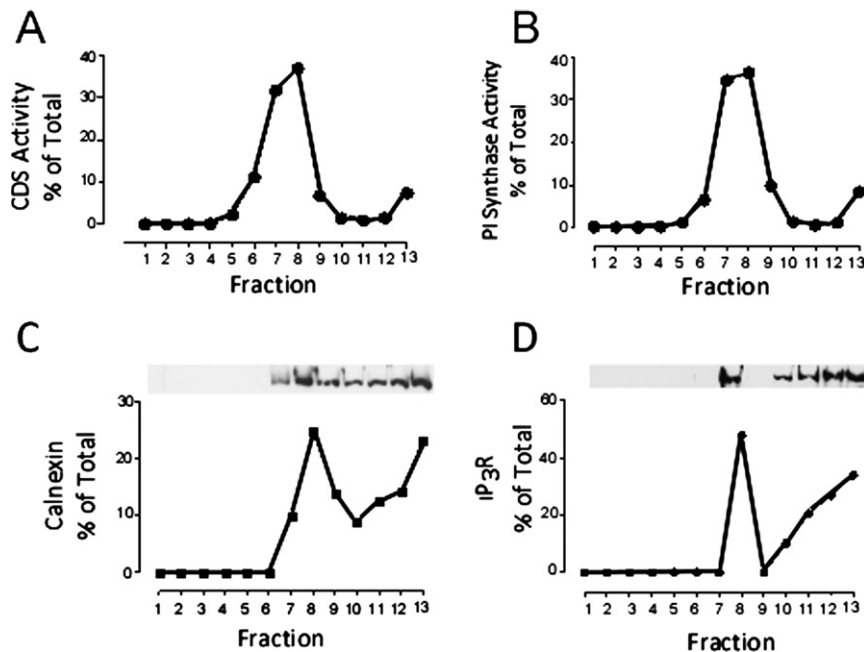


Fig. 4. Fragmentation of ER membranes by probe sonication and density gradient separation at neutral pH reveals differences in the distributions of CDP-DAG and PI synthesis compared with calnexin and IP₃R. A431 cells were harvested by scraping into neutral pH buffer, probe sonicated, and membranes separated on a 45-35-20-5% (w/v) sucrose discontinuous density gradient. One milliliter gradient fractions were then harvested beginning from the top of the tube for further analysis. Distributions of (A) [³²P]CDP-DAG (total cpm 29,228) and (B) [³H]PI synthesis (total dpm 205,590) generation in the gradient fractions. Immunoblots and densitometric analyses of (C) calnexin and (D) IP₃R distributions in the gradient fractions. Data are representative of two independent experiments.

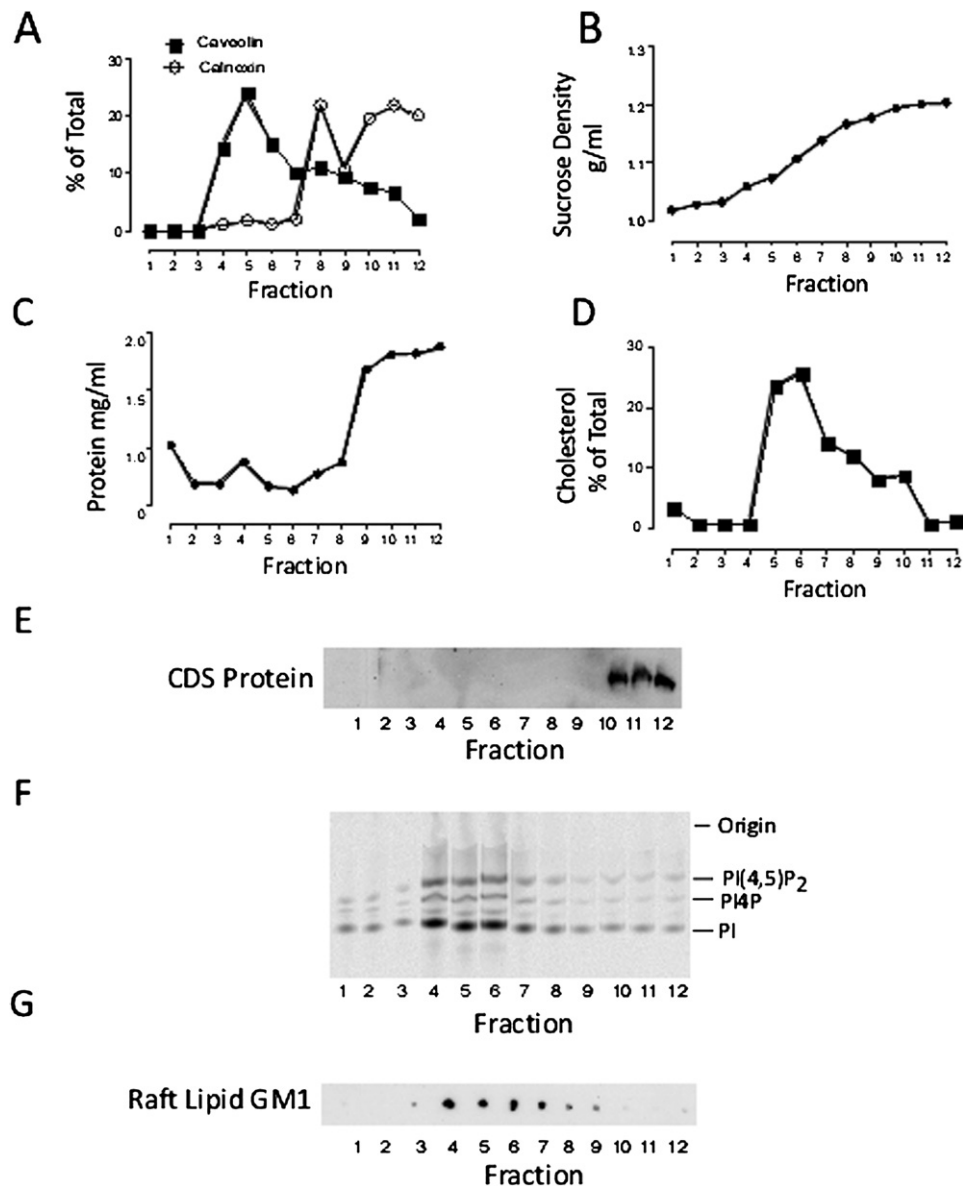


Fig. 5. Unlike caveolae lipid rafts, calnexin, and CDP-DAG synthesizing membrane domains are soluble in detergent. Cells were harvested and sonicated in the presence of 0.1M sodium carbonate, and the detergents β -octylglucoside (10 mM) and deoxycholate (4 mM) and the homogenate centrifuged in a 45-35-5% (w/v) sucrose discontinuous density gradient. Fractions 5 and 6 correspond to the interface of the 5 and 35% sucrose layer. A: Densitometric analysis comparing the distributions of caveolin and calnexin in the gradient as determined by immunoblotting. B: Sucrose density profile of a 45-35-5% (w/v) sucrose gradient. C: Protein content of the gradient fractions measured using the Bradford assay. D: Distribution of cholesterol in the gradient fractions determined by the Amplex Red cholesterol mass assay. E: Immunoblot showing the distribution of CDS protein in the gradient fractions. F: TLC separation of [3 H]inositol labeled phospholipids in the gradient fractions G: Dot-blot showing distribution of GM1 glycosphingolipid in the gradient fractions. Each data panel shown is representative of at least two independent measurements from three subcellular fractionation experiments.

CDS and calnexin were unevenly distributed throughout the ER with colocalization in 1–2 μ m patches, often adjacent to membrane domains staining for only one or other of these proteins (Fig. 6, detail 1). There were also distinct patches of colocalization at the plasma membrane although this was less extensive than at the ER (Fig. 6, detail 2). This patchwork of separate and overlapping localization could be seen more clearly in higher resolution images (Fig. 6). Our confocal microscope is

routinely calibrated with dye-labeled Tetraspeck beads (Life Technologies) using the same objective and acquisition settings. This gives an x-y resolution of at least 200–250 nm at these emission wavelengths, figures that closely correspond to calculations of theoretical diffraction-limited resolution. Given this level of imaging resolution, it is accurate to imply that calnexin and CDS colocalize in membrane microdomains. These results are consistent with the membrane immunoisolation and

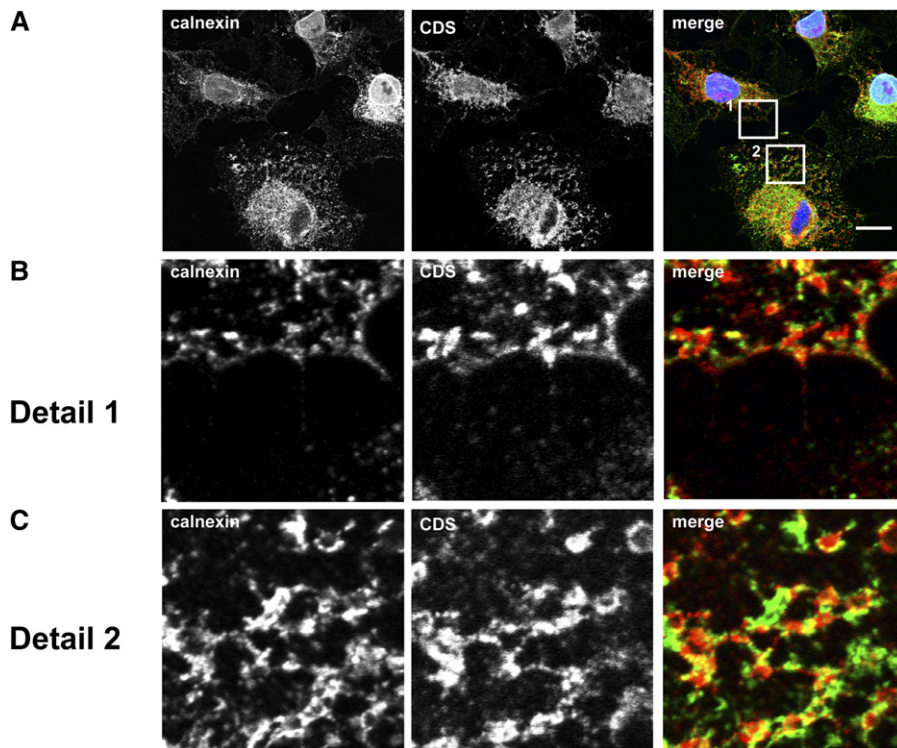


Fig. 6. ER and plasma membrane microdomains enriched for calnexin and CDS. A: Cells grown on coverslips were fixed and permeabilized in methanol and immunostained with anti-calnexin (green) and anti-CDS (red) antibodies. B: Detail of calnexin and CDS localization at the plasma membrane. C: Zoomed image showing overlap between calnexin and CDS on membrane patches on reticular membranes. Scale bar is 10 μ M. Images are representative of three independent experiments.

cell fractionation data demonstrating that cellular CDS activity is concentrated in calnexin-rich membrane microdomains.

DISCUSSION

Through the use of a variety of cell fractionation, immunoprecipitation, and immunofluorescence imaging techniques, we demonstrated that a pool of CDS activity localizes to calnexin-containing ER membrane domains that cofractionate with low-buoyant density caveolae but with biochemical properties that are different to those ascribed to plasma membrane rafts. Specifically, the novel phospholipid-synthesizing membrane domains we describe here are detergent-soluble and are not enriched for either cholesterol or glycosphingolipids. This sets them apart from the detergent-resistant ER domains implicated in the synthesis of mammalian glycosylphosphatidylinositol anchor intermediates (54), the organization of export to the Golgi (55), and also from the detergent-insoluble membrane domains to which erlin-1/2 (7) and sigma-1 chaperones (6) are targeted.


Another novel finding from our coimmunoprecipitation studies is the origin of the CDP-DAG-synthesizing domains in the calnexin and type III IP₃R-containing region of ER. We have shown on a number of previous occasions that the sonication procedure we use to disrupt the ER membranes gives rise to membrane vesicles in the size range of 60–200 nm diameter (32, 48, 49); hence, the ability

to coimmunoprecipitate calnexin, IP₃R and CDS on intact vesicles demonstrates that these proteins localize in the same microdomain of the ER. The differential localizations of CDP-DAG synthesis, calnexin, and type III IP₃R do not become apparent in subcellular fractionation experiments until these ER membranes are sonicated and this is most pronounced when membranes are sonicated using neutral pH buffer. Moreover, the differing equilibrium densities and partial overlaps of CDS, calnexin, and IP₃R in the density gradient fractions following sonication indicate a substantial degree of membrane domain heterogeneity within the ER.

The low buoyancy of phospholipid-rich membrane domains in neutral pH buffer is indicative of a high protein-to-lipid ratio under physiological conditions. The density shift of these membranes apparent following carbonate treatment indicates that peripherally associated proteins account for the lack of buoyancy in neutral pH buffer (51). This differs from cholesterol-rich membranes at other cellular sites, such as the *trans*-Golgi network, which tend to be intrinsically buoyant due to their relatively low protein-to-lipid ratio (56). The low abundance of cholesterol at the ER, which is a tightly regulated process (57), and the exclusion of cholesterol from model membranes containing unsaturated lipid side chains (58, 59) further argue against a predominant role for classical lipid raft domains in the organization of phospholipid synthesis. The membrane microdomains that we describe here appear to have the properties expected of the so-called

“non-raft” phospholipid-rich membrane domains, the existence of which was first postulated by Shaikh and Edidin (35). To the best of our knowledge, this is the first experimental evidence that such membrane domains exist in cells and furthermore, our results indicate that these domains are an important site for cellular phospholipid synthesis.

Our analyses of the biochemical and membrane fraction data is supported by confocal microscopy, which demonstrates that CDS and calnexin colocalize in micron-sized patches of membrane but that there are also portions of the ER where there is no overlap between these proteins. This is somewhat unexpected as ER membranes are generally thought to mainly exist in a liquid disordered state due to a lipid composition that is conducive to neither phase separation nor membrane microdomain formation. However, our visualization of a small pool of CDS-calnexin very close to or on the plasma membrane may indicate that inter-membrane and inter-protein contacts could have a role in the formation and/or stabilization of these ER microdomains. The presence of a small pool of calnexin at the plasma membrane has been reported in several previous studies (8, 60, 61) and is dependent on CK2 phosphorylation and inhibition of PACS-2 binding to calnexin (8). This implies that the subcellular localization of the CDS-calnexin domain may not be static and opens the possibility of a trafficking route whereby CDS and IP₃R can cotraffic with phosphorylated calnexin to the plasma membrane (8). Localization of CDS extremely close to or definitively on the plasma membrane has ramifications for the long-running puzzle concerning possible spatial restrictions to phosphoinositide substrate supply, which would arise if CDP-DAG synthesis was exclusively compartmentalized at the ER. Our observations may indicate that local rates of CDP-DAG synthesis and the abundance of CDS in a particular membrane environment may be key factors in regulating the supply of PI at the plasma membrane.

In conclusion, our results demonstrate that a pool of IP₃R associates with membrane microdomains that are highly enriched for calnexin and CDP-DAG synthesis. Future work will determine the functional consequences of CDS targeting to these novel membrane regions, including the pool of the enzyme we have imaged at the plasma membrane. Because IP₃R and CDS are key proteins in receptor-dependent phosphoinositide signaling, it is possible that the membrane domains we have identified here are important for the spatial integration of phospholipid synthesis with the propagation of signaling from phosphoinositide-derived second messengers. It is noteworthy that calnexin is a Ca²⁺ binding protein that can function as a low-affinity high-capacity Ca²⁺ buffer (62-64) and also that CDP-DAG generation in cells is inhibited by mM Ca²⁺ concentrations (27). Therefore, we speculate that the close proximities of calnexin, IP₃R, and CDS may facilitate the localized coupling of Ca²⁺ release with compensatory PI resynthesis via calnexin-mediated buffering of Ca²⁺ increases close to the ER membrane. 

We thank Samrina Aslam for her assistance with the imaging studies.

REFERENCES

- Pike, L. J. 2003. Lipid rafts: bringing order to chaos. *J. Lipid Res.* **44**: 655–667.
- Pike, L. J. 2004. Lipid rafts: heterogeneity on the high seas. *Biochem. J.* **378**: 281–292.
- Fagone, P., and S. Jackowski. 2009. Membrane phospholipid synthesis and endoplasmic reticulum function. *J. Lipid Res.* **50**(Suppl): S311–S316.
- Hayashi, T., R. Rizzuto, G. Hajnoczky, and T. P. Su. 2009. MAM: more than just a housekeeper. *Trends Cell Biol.* **19**: 81–88.
- Vance, J. E. 1990. Phospholipid synthesis in a membrane fraction associated with mitochondria. *J. Biol. Chem.* **265**: 7248–7256.
- Hayashi, T., and M. Fujimoto. 2010. Detergent-resistant microdomains determine the localization of sigma-1 receptors to the endoplasmic reticulum-mitochondria junction. *Mol. Pharmacol.* **77**: 517–528.
- Browman, D. T., M. E. Resek, L. D. Zajchowski, and S. M. Robbins. 2006. Erlin-1 and erlin-2 are novel members of the prohibitin family of proteins that define lipid-raft-like domains of the ER. *J. Cell Sci.* **119**: 3149–3160.
- Myhill, N., E. M. Lynes, J. A. Nanji, A. D. Blagoveshchenskaya, H. Fei, K. Carmine Simmen, T. J. Cooper, G. Thomas, and T. Simmen. 2008. The subcellular distribution of calnexin is mediated by PACS-2. *Mol. Biol. Cell.* **19**: 2777–2788.
- Mendes, C. C., D. A. Gomes, M. Thompson, N. C. Souto, T. S. Goes, A. M. Goes, M. A. Rodrigues, M. V. Gomez, M. H. Nathanson, and M. F. Leite. 2005. The type III inositol 1,4,5-trisphosphate receptor preferentially transmits apoptotic Ca²⁺ signals into mitochondria. *J. Biol. Chem.* **280**: 40892–40900.
- Hayashi, T., and T. P. Su. 2007. Sigma-1 receptor chaperones at the ER-mitochondrion interface regulate Ca(2+) signaling and cell survival. *Cell.* **131**: 596–610.
- Monaco, M. E., and M. C. Gershengorn. 1992. Subcellular organization of receptor-mediated phosphoinositide turnover. *Endocr. Rev.* **13**: 707–718.
- Michell, R. H. 1975. Inositol phospholipids and cell surface receptor function. *Biochim. Biophys. Acta.* **415**: 81–147.
- Kirk, C. J., P. A. Hunt, and R. H. Michell. 1989. Do cells contain discrete pools of inositol lipids that are coupled to receptor activation? *Biochem. Soc. Trans.* **17**: 978–980.
- Batty, I. H., R. A. Currie, and C. P. Downes. 1998. Evidence for a model of integrated inositol phospholipid pools implies an essential role for lipid transport in the maintenance of receptor-mediated phospholipase C activity in 1321N1 cells. *Biochem. J.* **330**: 1069–1077.
- Monaco, M. E. 1987. Inositol metabolism in WRK-1 cells. Relationship of hormone-sensitive to -insensitive pools of phosphoinositides. *J. Biol. Chem.* **262**: 13001–13006.
- Whatmore, J., C. Wiedemann, P. Somerharju, P. Swigart, and S. Cockcroft. 1999. Resynthesis of phosphatidylinositol in permeabilized neutrophils following phospholipase C β activation: transport of the intermediate, phosphatidic acid, from the plasma membrane to the endoplasmic reticulum for phosphatidylinositol resynthesis is not dependent on soluble lipid carriers or vesicular transport. *Biochem. J.* **341**: 435–444.
- Heacock, A. M., and B. W. Agranoff. 1997. CDP-diacylglycerol synthase from mammalian tissues. *Biochim. Biophys. Acta.* **1348**: 166–172.
- Antonsson, B. 1997. Phosphatidylinositol synthase from mammalian tissues. *Biochim. Biophys. Acta.* **1348**: 179–186.
- Vaziri, C., C. P. Downes, and S. C. Macfarlane. 1993. Direct labeling of hormone-sensitive phosphoinositides by a plasma-membrane-associated PtdIns synthase in turkey erythrocytes. *Biochem. J.* **294**: 793–799.
- Imai, A., and M. C. Gershengorn. 1987. Independent phosphatidylinositol synthesis in pituitary plasma membrane and endoplasmic reticulum. *Nature.* **325**: 726–728.
- Williamson, F. A., and D. J. Morre. 1976. Distribution of phosphatidylinositol biosynthetic activities among cell fractions from rat liver. *Biochem. Biophys. Res. Commun.* **68**: 1201–1205.
- Lykidis, A., P. D. Jackson, C. O. Rock, and S. Jackowski. 1997. The role of CDP-diacylglycerol synthetase and phosphatidylinositol synthase activity levels in the regulation of cellular phosphatidylinositol content. *J. Biol. Chem.* **272**: 33402–33409.
- Carter, J. R., and E. P. Kennedy. 1966. Enzymatic synthesis of cytidine diphosphate diglyceride. *J. Lipid Res.* **7**: 678–683.

24. Jelsema, C. L., and D. J. Morre. 1978. Distribution of phospholipid biosynthetic enzymes among cell components of rat liver. *J. Biol. Chem.* **253**: 7960–7971.
25. Liteplo, R. G., and M. Sribney. 1980. The stimulation of rat liver microsomal CTP: phosphatidate cytidyltransferase activity by guanosine triphosphate. *Biochim. Biophys. Acta.* **619**: 660–668.
26. Saito, S., K. Goto, A. Tonosaki, and H. Kondo. 1997. Gene cloning and characterization of CDP-diacylglycerol synthase from rat brain. *J. Biol. Chem.* **272**: 9503–9509.
27. Claro, E., J. N. Fain, and F. Picatoste. 1993. Noradrenaline stimulation unbalances the phosphoinositide cycle in rat cerebral cortical slices. *J. Neurochem.* **60**: 2078–2086.
28. Kasinathan, C., and M. A. Kirchberger. 1988. Presence of a Ca²⁺-sensitive CDPdiglyceride-inositol transferase in canine cardiac sarcoplasmic reticulum. *Biochemistry.* **27**: 2834–2839.
29. Claro, E., M. A. Wallace, and J. N. Fain. 1992. Concerted CMP-dependent [³H]inositol labeling of phosphoinositides and agonist activation of phospholipase C in rat brain cortical membranes. *J. Neurochem.* **58**: 2155–2161.
30. Bush, K. T., R. O. Stuart, S. H. Li, L. A. Moura, A. H. Sharp, C. A. Ross, and S. K. Nigam. 1994. Epithelial inositol 1,4,5-trisphosphate receptors. Multiplicity of localization, solubility, and isoforms. *J. Biol. Chem.* **269**: 23694–23699.
31. Schnitzer, J. E., P. Oh, B. S. Jacobson, and A. M. Dvorak. 1995. Caveolae from luminal plasmalemma of rat lung endothelium: microdomains enriched in caveolin, Ca(2+)-ATPase, and inositol trisphosphate receptor. *Proc. Natl. Acad. Sci. USA.* **92**: 1759–1763.
32. Waugh, M. G., D. Lawson, S. K. Tan, and J. J. Hsuan. 1998. Phosphatidylinositol 4-phosphate synthesis in immunisolated caveolae-like vesicles and low buoyant density non-caveolar membranes. *J. Biol. Chem.* **273**: 17115–17121.
33. Stan, R. V., W. G. Roberts, D. Predescu, K. Ihida, L. Saucan, L. Ghitescu, and G. E. Palade. 1997. Immunolocalization and partial characterization of endothelial plasmalemmal vesicles (caveolae). *Mol. Biol. Cell.* **8**: 595–605.
34. Sevlever, D., S. Pickett, K. J. Mann, K. Sambamurti, M. E. Medof, and T. L. Rosenberry. 1999. Glycosylphosphatidylinositol-anchor intermediates associate with triton-insoluble membranes in subcellular compartments that include the endoplasmic reticulum. *Biochem. J.* **343**: 627–635.
35. Shaikh, S. R., and M. A. Eddidin. 2006. Membranes are not just rafts. *Chem. Phys. Lipids.* **144**: 1–3.
36. Silience, D. J., and C. P. Downes. 1993. Subcellular distribution of agonist-stimulated phosphatidylinositol synthesis in 1321 N1 astrocytoma cells. *Biochem. J.* **290**: 381–387.
37. Dawson, R. M. C., D. C. Elliot, W. H. Elliot, and K. M. Jones. 1986. Data for Biochemical Research. 3rd edition. Oxford Science Publications.
38. Song, K. S., S. Li, T. Okamoto, L. A. Quilliam, M. Sargiacomo, and M. P. Lisanti. 1996. Co-purification and direct interaction of Ras with caveolin, an integral membrane protein of caveolae microdomains. Detergent-free purification of caveolae microdomains. *J. Biol. Chem.* **271**: 9690–9697.
39. Waugh, M. G., S. Minogue, D. Blumenkrantz, J. S. Anderson, and J. J. Hsuan. 2003. Identification and characterization of differentially active pools of type IIalpha phosphatidylinositol 4-kinase activity in unstimulated A431 cells. *Biochem. J.* **376**: 497–503.
40. Mok, A. Y., G. E. McDougall, and W. C. McMurray. 1992. CDP-diacylglycerol synthesis in rat liver mitochondria. *FEBS Lett.* **312**: 236–240.
41. Ilangumaran, S., S. Arni, Y. Chicheportiche, A. Briol, and D. C. Hoessli. 1996. Evaluation by dot-immunoassay of the differential distribution of cell surface and intracellular proteins in glycosylphosphatidylinositol-rich plasma membrane domains. *Anal. Biochem.* **235**: 49–56.
42. Minogue, S., M. G. Waugh, M. A. De Matteis, D. J. Stephens, F. Berditchevski, and J. J. Hsuan. 2006. Phosphatidylinositol 4-kinase is required for endosomal trafficking and degradation of the EGF receptor. *J. Cell Sci.* **119**: 571–581.
43. Rothberg, K. G., J. E. Heuser, W. C. Donzell, Y. S. Ying, J. R. Glenney, and R. G. Anderson. 1992. Caveolin, a protein component of caveolae membrane coats. *Cell.* **68**: 673–682.
44. Glenney, J. R., Jr., and D. Soppet. 1992. Sequence and expression of caveolin, a protein component of caveolae plasma membrane domains phosphorylated on tyrosine in Rous sarcoma virus-transformed fibroblasts. *Proc. Natl. Acad. Sci. USA.* **89**: 10517–10521.
45. Dupree, P., R. G. Parton, G. Raposo, T. V. Kurzchalia, and K. Simons. 1993. Caveolae and sorting in the trans-Golgi network of epithelial cells. *EMBO J.* **12**: 1597–1605.
46. Robenek, M. J., N. J. Severs, K. Schlattmann, G. Plenz, K. P. Zimmer, D. Troyer, and H. Robenek. 2004. Lipids partition caveolin-1 from ER membranes into lipid droplets: updating the model of lipid droplet biogenesis. *FASEB J.* **18**: 866–868.
47. Waugh, M. G., and J. J. Hsuan. 2009. Preparation of membrane rafts. *Methods Mol. Biol.* **462**: 403–414.
48. Waugh, M. G., D. Lawson, and J. J. Hsuan. 1999. Epidermal growth factor receptor activation is localized within low-buoyant density, non-caveolar membrane domains. *Biochem. J.* **337**: 591–597.
49. Waugh, M. G., K. M. Chu, E. L. Clayton, S. Minogue, and J. J. Hsuan. 2011. Detergent-free isolation and characterization of cholesterol-rich membrane domains from trans-Golgi network vesicles. *J. Lipid Res.* **52**: 582–589.
50. Pike, L. J., and J. M. Miller. 1998. Cholesterol depletion delocalizes phosphatidylinositol bisphosphate and inhibits hormone-stimulated phosphatidylinositol turnover. *J. Biol. Chem.* **273**: 22298–22304.
51. Fujiki, Y., A. L. Hubbard, S. Fowler, and P. B. Lazarow. 1982. Isolation of intracellular membranes by means of sodium carbonate treatment: application to endoplasmic reticulum. *J. Cell Biol.* **93**: 97–102.
52. Waugh, M. G., S. Minogue, J. S. Anderson, A. Balinger, D. Blumenkrantz, D. P. Calnan, R. Cramer, and J. J. Hsuan. 2003. Localization of a highly active pool of type II phosphatidylinositol 4-kinase in a p97/valosin-containing-protein-rich fraction of the endoplasmic reticulum. *Biochem. J.* **373**: 57–63.
53. Bishop, H. H., and K. P. Strickland. 1976. Studies on the formation by rat brain preparations of CDP-diglyceride from CTP and phosphatidic acids of varying fatty acid compositions. *Can. J. Biochem.* **54**: 249–260.
54. Pielsticker, L. K., K. J. Mann, W. L. Lin, and D. Sevlever. 2005. Raft-like membrane domains contain enzymatic activities involved in the synthesis of mammalian glycosylphosphatidylinositol anchor intermediates. *Biochem. Biophys. Res. Commun.* **330**: 163–171.
55. Bonnon, C., M. W. Wendeler, J. P. Paccard, and H. P. Hauri. 2010. Selective export of human GPI-anchored proteins from the endoplasmic reticulum. *J. Cell Sci.* **123**: 1705–1715.
56. Waugh, M. G., K. M. Chu, E. L. Clayton, S. Minogue, and J. J. Hsuan. 2011. Detergent-free isolation and characterization of cholesterol-rich membrane domains from trans-Golgi network vesicles. *J. Lipid Res.* **52**: 582–589.
57. Radhakrishnan, A., J. L. Goldstein, J. G. McDonald, and M. S. Brown. 2008. Switch-like control of SREBP-2 transport triggered by small changes in ER cholesterol: a delicate balance. *Cell Metab.* **8**: 512–521.
58. Shaikh, S. R., V. Cherezov, M. Caffrey, W. Stillwell, and S. R. Wassall. 2003. Interaction of cholesterol with a docosahexaenoic acid-containing phosphatidylethanolamine: trigger for microdomain/raft formation? *Biochemistry.* **42**: 12028–12037.
59. Shaikh, S. R., A. C. Dumauval, A. Castillo, D. LoCascio, R. A. Siddiqui, W. Stillwell, and S. R. Wassall. 2004. Oleic and docosahexaenoic acid differentially phase separate from lipid raft molecules: a comparative NMR, DSC, AFM, and detergent extraction study. *Biophys. J.* **87**: 1752–1766.
60. Wiest, D. L., W. H. Burgess, D. McKean, K. P. Kearse, and A. Singer. 1995. The molecular chaperone calnexin is expressed on the surface of immature thymocytes in association with clonotype-independent CD3 complexes. *EMBO J.* **14**: 3425–3433.
61. Okazaki, Y., H. Ohno, K. Takase, T. Ochiai, and T. Saito. 2000. Cell surface expression of calnexin, a molecular chaperone in the endoplasmic reticulum. *J. Biol. Chem.* **275**: 35751–35758.
62. Schrag, J. D., J. J. Bergeron, Y. Li, S. Borisova, M. Hahn, D. Y. Thomas, and M. Cygler. 2001. The structure of calnexin, an ER chaperone involved in quality control of protein folding. *Mol. Cell.* **8**: 633–644.
63. Tjoelker, L. W., C. E. Seyfried, R. L. Eddy, Jr., M. G. Byers, T. B. Shows, J. Calderon, R. B. Schreiber, and P. W. Gray. 1994. Human, mouse, and rat calnexin cDNA cloning: identification of potential calcium binding motifs and gene localization to human chromosome 5. *Biochemistry.* **33**: 3229–3236.
64. Rosenbaum, E. E., R. C. Hardie, and N. J. Colley. 2006. Calnexin is essential for rhodopsin maturation, Ca²⁺ regulation, and photoreceptor cell survival. *Neuron.* **49**: 229–241.